Hyperbranched Block Copolymer from AB_2 Macromonomer: Synthesis and Its Reaction-Induced Microphase Separation in Epoxy Thermosets

Jingang Li, Yixin Xiang, Sixun Zheng

Department of Polymer Science and Engineering and the State Key Laboratory of Metal Matrix Composites, Shanghai Jiao Tong University, Shanghai 200240, People's Republic of China
Correspondence to: S. Zheng (E-mail: szheng@sjtu.edu.cn)

Received 1 June 2015; accepted 11 July 2015; published online 6 August 2015
DOI: 10.1002/pola.27784

ABSTRACT: In this contribution, we reported the synthesis of a hyperbranched block copolymer composed of poly(ε-caprolactone) (PCL) and polystyrene (PS) subchains. Toward this end, we first synthesized an α-alkynyl- and ω,ω′-diazido-terminated PCL-*b*-$(PS)_2$ macromonomer *via* the combination of ring-opening polymerization and atom transfer radical polymerization. By the use of this AB_2 macromonomer, the hyperbranched block copolymer (*h*-[PCL-*b*-$(PS)_2$]) was synthesized via a copper-catalyzed Huisgen 1,3-dipolar cycloaddition (i.e., click reaction) polymerization. The hyperbranched block copolymer was characterized by means of ^1H nuclear magnetic resonance spectroscopy and gel permeation chromatography. Both differential scanning calorimetry and atomic force microscopy showed that the hyperbranched block copolymer was microphase-separated in bulk. While this hyperbranched block copolymer was incorporated into epoxy, the nanostructured thermosets were successfully obtained; the formation of the nanophases in epoxy followed reaction-induced microphase separation mechanism as evidenced by atomic force microscopy, small angle X-ray scattering, and dynamic mechanical thermal analysis. © 2015 Wiley Periodicals, Inc. J. Polym. Sci., Part A: Polym. Chem. **2016**, *54*, 368–380

KEYWORDS: block copolymer; ring-opening polymerization; atom transfer radical polymerization

INTRODUCTION Hyperbranched polymers are a class of important materials, which have special physical and chemical properties due to their highly branched architecture and high numbers of functional end groups; they have been used as specialty coating, nanostructured network and for various biomedical applications.[1–5] Hyperbranched polymers can be synthesized by the use of a series of functional monomers.[4] Depending on types of monomers and polymerizations, hyperbranched polymers can display a variety of structure and properties. Of them, hyperbranched polymers resulting from AB_2 type monomers have attracted considerable interest.[6–11] In 1995, Fréchet et al. reported the self-condensing vinyl or ring-opening polymerization (SCVP or SCROP) of AB_2 monomers.[12–17] For SCVP, hyperbranched chains are formed via polymerization of vinyl monomers with an initiating group. In SCROP reaction, an AB_2 monomer contains a polymerizable cyclic group instead of vinyl group in an SCVP monomer. Similar to low molecule AB_2 monomers, Y-shaped AB_2 macromonomers with long subchains can also be used to obtain hyperbranched polymers via self-polymerization approach (See Scheme 1). For instance, Hedrick and coworkers[18] synthesized hyperbranched poly(ε-caprolactone)s by the use of a short-chain PCL macromonomer with one carboxylic acid end and two hydroxyl groups at the other ends via polycondensation. Depending on types of short chains and end groups, a variety of hyperbranched polymers with fairly long repeat units have been synthesized via different self-polymerization approaches.[6–17] In most of the previous reports, such hyperbranched polymers are homopolymers. Occasionally, hyperbranched block copolymers were synthesized. Hedrick and coworkers[18] reported the synthesis of a series of hyperbranched block copolymers by using the polycondensation copolymerization of different AB_2 macromonomers bearing terminal carboxyl and hydroxyl groups. More recently, Li et al.[19] reported the synthesis of amphiphilic hyperbranched block copolymers via a grafting-to approach. They first synthesized the hyperbranched poly(acrylic acid) (or polystyrene) homopolymers with a great number of azido end groups; then mono-alkynyl-terminated polystyrene (PS) [or poly(acrylic acid)] was grafted onto the hyperbranched polymer via a copper-catalyzed Huisgen 1,3-dipolar cycloaddition reaction.

It has been realized that incorporating amphiphilic block copolymers into thermosetting polymers can obtain the nanostructured thermosets with improved mechanical and functional properties.[20–49] It is found that the formation of the nanophases in thermosets can follow self-assembly[20,21]

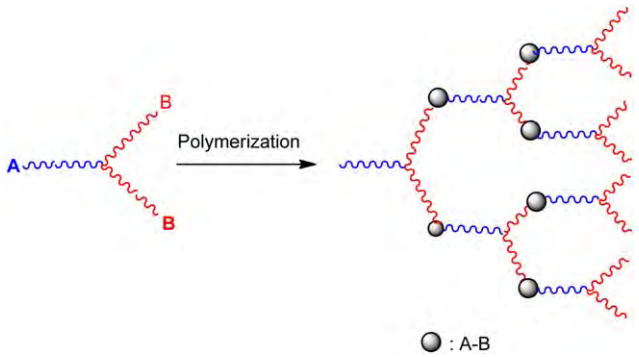

SCHEME 1 An AB2 macromonomer and its hyperbranched block copolymer via step-growth polymerization. [Color figure can be viewed in the online issue, which is available at wileyonlinelibrary.com.]

or reaction-induced microphase separation[22,23] mechanism. The morphologies of nanophases in thermosets are quite dependent on the architecture of the block copolymers, the composition of the thermosets and the control over the curing process. In most of the previous studies, block copolymers with linear architectures are employed to create the nanophases in thermosets. Recently, the block copolymers with nonlinear architectures have been used to investigate the formation of the nanophases.[32,40,44,51] For instance, Serrano et al.[35,44] first reported the formation of ordered nanostructures in epoxy thermosets containing epoxidized star-shaped polystyrene-*block*-polybutadiene block copolymer. Meng et al.[40] found that with the identical composition and lengths of blocks, the block copolymers with linear and star-like topologies can create different morphologies of the nanophases in epoxy thermosets. Zhu et al.[50] reported the formation of vesicular nanophases in epoxy thermosets containing an organic–inorganic macrocyclic molecular brush with poly(ε-caprolactone) (PCL)-*block*-PS side chains. However, such an investigation remained largely unexplored. It is proposed that nonlinear architecture of block copolymers could exert additional variables to influence the morphologies of the nanophases. In addition, nonlinear block copolymers have low hydrodynamic volume compared to their linear analogs. The decreased hydrodynamic volume can alter the competitive kinetics between curing reaction and microphase separation and thus affect the morphologies of the microdomains. This effect is much pronounced for the formation of the nanophases via reaction-induced microphase separation mechanism. To the best of our knowledge, there has been no precedent report on the formation of the nanophases in thermosets containing hyperbranched block copolymer.

In this work, we first reported the synthesis of a hyperbranched block copolymer and then explored to use it to control the formation of the nanostructures in epoxy thermosets. The hyperbranched block copolymer used in this work is composed of PCL and PS subchains (denoted *h*-P[PCL-*b*-$(PS)_2$]). To synthesize this hyperbranched block copolymer, we first synthesized an α-alkynyl- and o,o′-diazido-terminated AB_2 macromonomer via the combination of ROP and atom transfer radical polymerization (ATRP). Thereafter, the hyperbranched block copolymer was synthesized via a copper-catalyzed Huisgen 1,3-dipolar cycloaddition (i.e., click reaction) polymerization of the AB_2 macromonomer. The hyperbranched block copolymer is designed and synthesized by knowing that: i) PCL is miscible with epoxy after and before curing[51,52] and ii) PS undergoes a reaction-induced phase separation in the blends with epoxy.[53,54] It is expected that a reaction-induced microphase separation will occur in the thermosets. It is of interest to investigate the influence of hyperbranched architecture of the block copolymer on the formation of PS microdomains in the epoxy thermosets.

EXPERIMENTAL

Materials

Styrene (St) was purchased from Shanghai Reagent, China and it was passed through a basic alumina column to remove the inhibitor before use. ε-Caprolactone (CL) was purchased from Fluka Co., Germany; prior to use, it was distilled over CaH_2 under decreased pressure. Propargyl alcohol was purchased from Xiya Chemical Reagent Co. China and it was distillated before use. Stannous (II) octanoate [$Sn(Oct)_2$], 4-dimethylaminopyridine (DMAP), copper (I) bromide (CuBr) and 2-bromoisobutyryl bromide were of chemically pure grade, purchased from Shanghai Reagent Co., China. *N,N,N′,N′,N″*-Pentamethyldiethylenetriamine (PMDETA) were purchased from Aldrich Co., Shanghai, China and used as received. 1-(3-Dimethylaminopropyl)-3-ethylcarbodiimide hydrochloride (EDC) was of analytically pure grade, purchased from Aladdin Reagent Co., Shanghai, China. 2,2-Bis (hydroxymethyl)propionic acid, 2,2-dimethoxypropane and *p*-toluenesulfonic acid monohydrate are of chemically pure grade and purchased from Shanghai Reagent Co., China. Epoxy monomer used in this work is diglycidyl ether of bisphenol A (DGEBA), supplied by Shanghai Resin Co., China; it has a quoted epoxide equivalent weight of 185. 4,4′-Methylenebis(2-chloroaniline) (MOCA) is of chemically pure grade and was used as the curing agent, purchased from Shanghai Reagent, China. The organic solvents such as tetrahydrofuran (THF), triethylamine (TEA), *N,N*-dimethylformamide (DMF), methanol and dichloromethane (DCM) were of chemically pure grade, obtained from commercial sources. Before use, THF was refluxed over sodium and then distilled. TEA and DCM were refluxed over CaH_2 and then distilled. All other reagents and solvents used in this work are obtained from commercial resources and were purified according to standard procedures prior to use.

Synthesis of Isopropylidene-2,2-Bis(Methoxy) Propionic Acid

Isopropylidene-2,2-bis(methoxy)propionic acid was prepared in this lab by following the method of literature.[55] To a flask equipped with a magnetic stirrer, 2,2-bis(hydroxymethyl)propionic acid (15.000 g, 111.8 mmol), 2,2-dimethoxypropane (20.7 mL, 167.7 mmol), *p*-toluenesulfonic acid monohydrate (1.050 g, 5.5 mmol) and 40 mL of acetone were charged

with vigorous stirring. The reaction was carried out at room temperature for 5 h and then the mixture of 0.4 mL ammonia solution (25%) with 0.4 mL ethanol was added with vigorous stirring for 5 min; the acetone was removed via rotary evaporation and 250 mL of DCM was added to dissolve the residue. The mixture was washed with deionized water (50 mL × 3). The organic layer was collected and then dried over anhydrous MgSO4 for 24 h. After filtration, the solvent of filtrate was removed via rotary evaporation and the white powder (13.28 g) was obtained with the yield of 80.5%. ^{1}H NMR ($CDCl_3$, ppm): 4.18, 3.65 [2H, -C***H***$_2$O(CH_3)C(CH_3)OC***H***$_2$-)], 1.41, 1.38 [6H, CH_2O(C***H***$_3$)C(C***H***$_3$)OCH_2], 1.20 [3H, C***H***$_3$C(CH_2O)$_2$COOH].

Synthesis of α-Alkynyl- and o-Hydroxyl-Terminated PCL

α-Alkynyl- and ω-hydroxyl-terminated poly(ε-caprolactone) (denoted alkynyl-PCL-OH) was synthesized via the ROP of CL with propargyl alcohol as initiator and with Sn(Oct)$_2$ as the catalyst. Typically, propargyl alcohol (0.465 g, 8.3 mmol), CL (20.0 g, 175.43 mmol) and Sn(Oct)$_2$ (20 mg) were charged to a flask equipped with a magnetic stirrer. The system was connected to a Schlenk line to degas via three pump-freeze-thaw cycles. The reaction was carried out at 100°C for 20 h. The crude product was dissolved in DCM and the solution was dropped into a great amount of methanol to afford the precipitates. The dissolution-precipitation procedure was repeated three times to purify the product. After dried at 30°C *in vacuo* for 24 h, the polymer (16.500 g) was obtained with the CL conversion of 82.5%. The molecular weight was estimated by ^{1}H NMR spectroscopy according to the ratio of the integral intensity of the peak at 4.0 ~ 4.1 ppm (-C***H***$_2$- in the main chain of PCL) to that at 3.64 ppm (HO-C***H***$_2$- at the chain end of PCL) to be M_n = 2300 Da. ^{1}H NMR ($CDCl_3$, ppm): 4.7 [2H, CH_2C***H***$_2$O], 4.05 [2H, OCO(CH_2)$_4$C***H***$_2$], 3.64 [2H, CH_2C***H***$_2$OH], 2.46 [1H, C***H***CCH_2], 2.30 [2H, OCOC***H***$_2$(CH_2)$_4$], 1.64 [4H, OCOCH_2C***H***$_2$CH_2C***H***$_2$CH_2], 1.39~1.37 [2H, OCOCH_2CH_2C***H***$_2$CH_2CH_2].

Synthesis of α-Alkynyl- and ω,ω′-Dibromo-Terminated PCL

First, the above alkynyl-PCL-OH (15.000 g, 6.52 mmol with respect of terminal hydroxyl group), isopropylidene-2,2-bis (methoxy)propionic acid (6.000 g, 34.5 mmol) and anhydrous DCM (50 mL) were charged to a flask equipped with a magnetic stirrer. At 0°C, 4-dimethylaminopyridine (DMAP) (210.5 mg, 1.73 mmol) and 1-(3-dimethylaminopropyl)-3-ethylcarbodiimide hydrochloride (EDC) (1.50 g, 7.824 mmol) were added to the flask with vigorous stirring. The reaction was carried out at 25°C for additional 48 h. The crude product was dropped into a great amount of methanol to afford the precipitates. The dissolution and precipitation procedure was repeated three times to purify the product. After drying at 30°C for 24 h, the α-alkynyl and ω-dioxane-terminated PCL (14.200 g) was obtained with the yield of 94.7%. ^{1}H NMR ($CDCl_3$, ppm): 4.7 [2H, CC***H***$_2$O], 4.05 [2H, OCO(CH_2)$_4$C***H***$_2$], 4.2, 3.7 [4H, OCOC(C***H***$_2$O)$_2$$CH_3$], 3.64 [2H, CH_2C***H***$_2$OH], 2.46 [1H, C***H***CCH_2], 2.30 [2H, OCOC***H***$_2$(CH_2)$_4$], 1.64 [4H, OCOCH_2 C***H***$_2$CH_2C***H***$_2$CH_2], 1.45–1.35 [8H, OCOCH_2CH_2C***H***$_2$CH_2CH_2, OC(C***H***$_3$)$_2$O], 1.2 [3H, OCOC(CH_2O)$_2$C***H***$_3$].

Second, the above α-alkynyl- and ω-dioxane-terminated PCL (denoted alkynyl-PCL-dioxane) (12.000 g, 5.22 mmol) was dissolved in 80 mL of anhydrous THF and then 2.7 mL of hydrochloric acid (1.0 M) was dropwise added. The mixture was stirred for 3.5 h at room temperature and then was diluted with 400 mL of DCM. The solution was washed with deionized water (40 mL × 2) and the organic layer was dried by adding anhydrous Na_2SO_4. The majority of solvent was eliminated via rotary evaporation; the concentrated solution was dropped into 350 mL of methanol to afford the precipitates. The procedure of dissolution and precipitation was repeated three times. After drying 30°C *in vacuo* overnight, the α-alkynyl- and o,o′-dihydroxyl-terminated PCL [alkynyl-PCL(OH)$_2$] (11.2 g) was obtained with the yield of 93.3%. ^{1}H NMR ($CDCl_3$, ppm): 4.7 [2H, CC***H***$_2$O], 4.05 [2H, OCO(CH_2)$_4$C***H***$_2$], 3.90, 3.74 [4H, OCOC(C***H***$_2$OH)$_2$$CH_3$], 3.64 [2H, CH_2C***H***$_2$OH], 2.46 [1H, C***H***CCH_2], 2.30 [2H, OCOC***H***$_2$(CH_2)$_4$], 1.64 [4H, OCOCH_2C***H***$_2$CH_2C***H***$_2$CH_2], 1.45–1.35 [2H, OCOCH_2CH_2C***H***$_2$CH_2 CH_2], 1.08 [3H, OCOC(CH_2O)$_2$C***H***$_3$].

Third, to a flask equipped with a magnetic stirrer, the above α-alkynyl- and ω,ω′-dihydroxyl-terminated PCL (10.500 g, 4.57 mmol) and 30 mL of DCM were charged with vigorous stirring. The flask was immersed into an ice-water bath and then 2-bromoisobutyryl bromide (3.0 mL, 24.27 mmol) and TEA (0.6 mL, 4.34 mmol) were added; the reaction was performed at room temperature for 24 h. The reacted mixture was dropped into 200 mL of methanol to afford the precipitates. The procedure of dissolution and precipitation was repeated three times to purify the product. After being dried at 30°C for 24 h, α-alkynyl- and ω,ω′-dibromo-terminated PCL [denoted alkynyl-PCL(Br)$_2$] (9.010 g) was obtained with the yield of 85.7%. ^{1}H NMR ($CDCl_3$, ppm): 4.7 [2H, CC***H***$_2$O], 4.4 (4H, COOC***H***$_2$), 4.05 [2H, OCO(CH_2)$_4$C***H***$_2$], 2.46 [1H, C***H***CCH_2], 2.30 [2H, OCOC***H***$_2$(CH_2)$_4$], 1.92 [12H, CBr(C***H***$_3$)$_2$], 1.64 [4H, OCOCH_2C***H***$_2$CH_2C***H***$_2$CH_2], 1.45–1.35 [5H, OCOCH_2CH_2C***H***$_2$CH_2 CH_2, OCOC(CH_2O)$_2$C***H***$_3$].

Synthesis of AB$_2$ Alkynyl-PCL-b-(PS-N$_3$)$_2$ Macromonomer

First, the α-alkynyl- and ω,ω′-dibromo-terminated poly(ε-caprolactone)-*block*-(polystyrene-Br)$_2$ [denoted alkynyl-PCL-*b*-(PS-Br)$_2$] was synthesized via the ATRP of styrene with the α-alkynyl and ω,ω′-dibromo-terminated poly(ε-caprolactone) as the initiator. Typically, the α-alkynyl and ω-dibromo-terminated poly(ε-caprolactone) (5.000 g, 2.17 mmol), St (115.000 g, 1.105 mol), Cu(I)Br (148.5 mg, 1.035 mmol) and PMDETA (210 μL, 1.035 mmol) were charged to a flask equipped with a magnetic stirrer. The system was connected to the Schlenk line and the system was degassed via three pump-freeze-thaw cycles. The polymerization was carried out at 60°C for 6 h to attain the desired conversion of styrene. The crude product was dissolved in THF and passed through a neutral alumina. After concentrated via rotary evaporation, the solution was dropped into a great amount of methanol to afford the precipitates. The procedure of dissolution and precipitation was repeated three times to purify the polymer. After dried in a vacuum oven at 30°C for 24 h, the polymer (11.500 g) was obtained by controlling the conversation of styrene to be about 5.7 %. GPC (DMF, PS

standard, RI detector): M_n = 5700 with M_w/M_n = 1.16; GPC (THF, light scattering detector): M_n = 4600 with M_w/M_n = 1.16. ^{1}H NMR ($CDCl_3$, ppm): 6.3 ~ 7.3 [5H, $C_6\boldsymbol{H}_5$], 4.7 [2H, $CC\boldsymbol{H}_2O$], 3.6 (4H, $COOC\boldsymbol{H}_2$), 4.05 [2H, $OCO(CH_2)_4C\boldsymbol{H}_2$], 2.46 [1H, $C\boldsymbol{H}CCH_2$], 2.30 [2H, $OCOC\boldsymbol{H}_2(CH_2)_4$], 1.64 [6H, $OCOCH_2C\boldsymbol{H}_2CH_2C\boldsymbol{H}_2CH_2$,$C\boldsymbol{H}_2CH(C_6H_5)$], 1.9 ~ 1.7 [H, $CH_2C\boldsymbol{H}(C_6H_5)$], 1.45 ~ 1.35 [5H, $OCOCH_2CH_2C\boldsymbol{H}_2CH_2CH_2$, $OCOC(CH_2O)_2C\boldsymbol{H}_3$], 0.90 [12H, $CBr(C\boldsymbol{H}_3)_2$].

Second, the above α-alkynyl- and ω,ω′-dibromo-terminated PCL-*b*-(PS-Br)$_2$ was reacted with sodium azide (NaN_3) to obtain the α-alkynyl and ω,ω′-diazido-terminated poly(ε-caprolactone)-*block*-(polystyrene-N_3)$_2$ block copolymer [denoted alkynyl-PCL-*b*-(PS-N_3)$_2$]. Typically, alkynyl-PCL-*b*-(PS-Br)$_2$ (10.000 g, 1.754 mmol), sodium azide (1.443 g, 19.1 mmol) and 40 mL of DMF were charged to a flask equipped with a magnetic stirrer. The reaction was carried out at 30°C for 48 h, and the reacted mixture was dropped into a great amount of mixture of deionized water with methanol (1/1, vol) to afford the precipitates; the dissolution-precipitation procedure was repeated three times. After drying at 30°C for 48 h, the product (9.420 g) was obtained with the yield of 94.2%. ^{1}H NMR ($CDCl_3$, ppm): 6.3–7.3 [5H, $C_6\boldsymbol{H}_5$], 4.7 [2H, $CC\boldsymbol{H}_2O$], 4.05 [2H, $OCO(CH_2)_4C\boldsymbol{H}_2$], 3.6 (4H, $COOC\boldsymbol{H}_2$), 2.46 [1H, $C\boldsymbol{H}CCH_2$], 2.30 [2H, $OCOC\boldsymbol{H}_2(CH_2)_4$], 1.64 [6H, $OCOCH_2C\boldsymbol{H}_2CH_2C\boldsymbol{H}_2CH_2$, $C\boldsymbol{H}_2CH(C_6H_5)$], 1.9–1.7 [H, $CH_2C\boldsymbol{H}(C_6H_5)$], 1.45-1.35 [5H, $OCOCH_2CH_2C\boldsymbol{H}_2CH_2CH_2$, $OCOC(CH_2O)_2C\boldsymbol{H}_3$], and 0.90 [12H, $CBr(C\boldsymbol{H}_3)_2$].

Synthesis of Hyperbranched Block Copolymer

The above α-alkynyl and ω,ω′-diazido-terminated alkynyl-PCL-*b*-(PS-N_3)$_2$ macromonomer was used to synthesize the hyperbranched block copolymer (denoted *h*-P[PCL-*b*-(PS)$_2$]) via copper-catalyzed Huisgen 1,3-dipolar cycloaddition (i.e., click reaction) polymerization. Typically, α-alkynyl and ω,ω′-diazido-terminated alkynyl-PCL-*b*-(PS-N_3)$_2$ macromonomer (9.000 g, 1.579 mmol), Cu(I)Br (453 mg, 3.158 mmol), PMDETA (660 uL, 3.158 mmol) and 30 mL of DMF were charged to a flask and the system was connected to the Schlenk line to degas via three pump-freeze-thaw cycles. The polymerization was carried out at 35°C for 72 h and the reacted mixture was dissolved in THF and passed through a neutral alumina to remove the catalyst. After concentration via rotary evaporation, the solution was dropped into a great amount of methanol to afford the precipitates. The product (8.200 g) was obtained with the yield of 91.1%. To remove the unreacted AB_2 macromonomer, the above product (8.0 g) was dissolved with 800 mL of DCM and then 250 mL of petroleum ether was dropped into the solution to obtain the white precipitates. The molecular weight was measured by gel permeation chromatography (GPC). GPC (DMF, PS standard, RI detector): M_n = 71,300 with the M_w/M_n = 1.43; GPC (THF, light scattering detector): M_n = 78,600 with M_w/M_n = 1.37. ^{1}H NMR ($CDCl_3$, ppm): 6.3 ~ 7.3 [5H, $C_6\boldsymbol{H}_5$], 4.05 [2H, $OCO(CH_2)_4C\boldsymbol{H}_2$], 3.6(4H, $COOC\boldsymbol{H}_2$), 2.30 [2H, $OCOC\boldsymbol{H}_2(CH_2)_4$], 1.64 [6H, $OCOCH_2C\boldsymbol{H}_2CH_2C\boldsymbol{H}_2CH_2$, $C\boldsymbol{H}_2CH(C_6H_5)$], 1.9~1.7 [H, $CH_2C\boldsymbol{H}(C_6H_5)$], 1.45–1.35 [5H, $OCOCH_2CH_2C\boldsymbol{H}_2CH_2CH_2$, $OCOC(CH_2O)_2C\boldsymbol{H}_3$], 0.90 [12H, $CN_3(C\boldsymbol{H}_3)_2$]

Preparation of Epoxy Thermosets

Desired amount of *h*-P[PCL-*b*-(PS)$_2$] was added to DGEBA at ambient temperature with continuous stirring until the system became homogeneous and transparent. Equimolar 4,4′-methylenebis(2-chloroaniline) (MOCA) with respect of the epoxide groups of the DGEBA was added to the mixture with vigorous stirring until the curing agent was fully dissolved. The ternary mixture was poured into Teflon molds to cure 150°C for 3 h plus 180°C for 2 h to obtain the thermosets. The thermosets containing *h*-P[PCL-*b*-(PS)$_2$] up to 40 wt % were prepared.

Measurement and Techniques

Nuclear Magnetic Resonance Spectroscopy

The ^{1}H nuclear magnetic resonance (NMR) measurement was carried out on a Varian Mercury Plus 400 MHz NMR spectrometer at 25°C. The samples were dissolved with deuterium chloroform and the solutions were measured with tetramethylsilane (TMS) as an internal reference.

Fourier Transform Infrared Spectroscopy

Fourier transform infrared spectroscopy (FTIR) spectroscopy was performed on a Perkin-Elmer Spectrum 1000 Fourier transform spectrometer at room temperature. The AB_2 macromonomer and hyperbranched block copolymer were dissolved in dichloromethane at the concentration of 5 wt % and the solutions were cast onto KBr windows. The majority of solvent was evaporated at room temperature and the residual solvent was removed *in vacuo* at 30°C for 2 h. The films of the samples were sufficiently thin to be within a range where the Beer-Lambert law is obeyed. In all cases 64 scans at a resolution of 2 cm^{-1} were used to record the spectra.

Gel Permeation Chromatography

The molecular weights and molecular weight distribution of polymers were measured on a Waters 1515 GPC system equipped with three Waters HR columns (HR4, HR3 and HR1). This apparatus was composed of an Isocratic HPLC pump and a RI detector. The measurements were carried out with *N*,*N*′-dimethylformamide (DMF) containing 0.01M LiBr as an eluent at the flow rate of 1.0 mL × min^{-1}. The molecular weight was expressed with PS standard. The molecular weights and molecular weight distribution of the AB2 macromonomer and hyperbranched block copolymer polymers were also measured on a Waters 717 Plus autosampler GPC apparatus equipped with Waters RH columns. This apparatus was equipped with a Dawn Eos (Wyatt Technology) multiangle laser light scattering detector; the measurements were carried out at 25°C with tetrahydrofuran (THF) as the eluent at the rate of 1.0 mL/min.

Atomic Force Microscopy

The specimens for atomic force microscopy (AFM) experiments were prepared via spin-coating the dichloromethane solution of *h*-P[PCL-*b*-(PS)$_2$] at the concentrations of 0.01 mg/mL onto silicon wafer at 2500 rpm. The solvent was evaporated at room temperature for 1 hour and the specimens were further dried *in vacuo* at room temperature for

30 min to eliminate the residual solvent. Prior to the morphological observation, the specimens were annealed at 30°C for 2 weeks and cooled to room temperature. The epoxy thermosets were trimmed on a microtome machine by the use of a diamond knife, and the thickness of the sections was about 200 nm. The morphological observation of the samples was conducted on a CSPM5500 nanoscope scanning probe microscope (Benyuan Instruments, Guangzhou, China) in tapping mode. A tip fabricated from silicon (125 μm in length with *c.a.* 500 kHz resonant frequency) was used for scan and the scan rate was 1.0 Hz.

Differential Scanning Calorimetry

Calorimetric measurements were performed on a TA Instruments Q2000 differential scanning calorimeter in a dry nitrogen atmosphere. The instrument was calibrated with a standard Indium. The samples (about 10.0 mg in weight) were first heated up to 120°C and held at this temperature for 3 min to eliminate thermal history, followed by quenching to −70°C. In all the cases, a heating rate of 20°C/min was used to record the heating thermograms. Glass transition temperature (T_g) was taken as the midpoint of heat capacity change.

Small-Angle X-ray Scattering

The small-angle X-ray scattering (SAXS) measurements were performed on a SAXS beamline of Shanghai Synchrotron Radiation Facility (SSRF), China. Two-dimensional diffraction patterns were recorded using an image intensified CCD detector. The experiments were carried out at room temperature (25°C) under condition of 8 keV photon energy and 300 nm small-angle resolutions. The intensity profiles were output as the plot of scattering intensity (I) versus scattering vector, $q = (4\pi/\lambda)\sin(\theta/2)$ (θ = scattering angle).

Dynamic Mechanical Thermal Analysis

The dynamic mechanical tests were performed on a TA Instruments DMA Q800 dynamic mechanical thermal analyzer (DMTA) equipped with a liquid nitrogen apparatus in a single cantilever mode. The frequency used was 3.0 Hz and the heating rate was 3.0°C/min. The specimen dimension was 1.2 × 2 × 0.1 cm^3. The experiments were carried out from −100°C until the specimens became too soft to be tested.

RESULTS AND DISCUSSION

Synthesis of AB_2 Macromonomer

The route of synthesis for the AB_2 macromonomer is shown in Scheme 2. First, an α-alkynyl- and ω-hydroxyl-terminated PCL [denoted alkynyl-PCL-OH] was synthesized via the ROP of ε-caprolactone with propargyl alcohol and stannous octanoate [$Sn(Oct)_2$] as the initiator and catalyst, respectively. The molecular weight of alkynyl-PCL-OH was controlled according to the molar ratio of propargyl alcohol to ε-caprolactone and the conversion of the monomer. Second, the esterification of the alkynyl-PCL-OH with isopropylidene-2,2-bis(methoxy)propionic acid was carried out to afford the α-alkynyl and ω-dioxane-terminated PCL (denoted alkynyl-PCL-dioxane). The deprotection of the terminal dioxane group was performed in the presence of hydrochloric acid to obtain an α-alkynyl and ω,ω′-dihydroxyl-terminated PCL [denoted alkynyl-PCL$(OH)_2$]. The alkynyl-PCL$(OH)_2$ was allowed to react with 2-bromoisobutyryl bromide to obtain an alkynyl- and ω,ω′-di(2-bromoisobutyryl)-terminated PCL [denoted alkynyl-PCL $(OOCC(CH_3)_2Br)_2$]. The latter was then used as the macromolecular initiator for the ATRP of styrene (St) to obtain alkynyl-PCL-*b*-$(PS\text{-}Br)_2$. The length of PS subchains was controlled by modulating the conversation of St. In the final step, the substitution reaction of alkynyl-PCL-*b*-$(PS\text{-}Br)_2$ with excess sodium azide (NaN_3) was carried out to afford the alkynyl-PCL-*b*-$(PS\text{-}N_3)_2$, which contained one alkynyl and two azido end groups, constituting a AB_2 macromonomer for the polymerization via copper-catalyzed Huisgen 1,3-dipolar cycloaddition reaction (i.e., click chemistry).

The ^1H NMR spectra of alkynyl-PCL-OH, alkynyl-PCL-dioxane, alkynyl-PCL$(OH)_2$, alkynyl-PCL$[OOCC(CH_3)_2Br]_2$, alkynyl-PCL-*b*-$(PS\text{-}Br)_2$ and alkynyl-PCL-*b*-$(PS\text{-}N_3)_2$ are shown in Figure 1. For alkynyl-PCL-OH, the signals of resonance at 1.35, 1.64, 2.29 and 4.06 ppm are assignable to the protons of methylene groups in the backbone of PCL chain. The signals of resonance at 2.46 and 4.57 ppm are attributable to the protons of methine and methylene in propargyl group. It should be pointed out that the signal of resonance at 3.64 ppm is attributable to the methylene protons of the hydroxymethyl groups at the end of PCL chain. According to the ratio of the integral intensity of this peak (at δ = 3.64 ppm assignable to the protons of ∼C$\boldsymbol{H}_2$OH) to other methylene protons in the backbone of PCL chains (e.g., at δ = 4.0 ∼ 4.1 ppm), the molecular weight of the PCL chain was calculated to be M_{PCL} = 2300 Da. For the alkynyl-PCL-dioxane, there appeared two new peaks at 1.19 and 4.16 ppm. The former is assignable to the protons of the methyl groups in the moiety of dioxane whereas the latter to the protons of methylene groups of the moiety. Besides the resonance at 4.16 ppm, the resonance of protons for the methylene groups in the moiety of dioxane was also detected at 3.63 and 4.19 ppm owing to the cyclic configuration of the dioxane. According to the ratio of the integral intensity of the resonance of the methyl protons at 1.19 ppm to those of methylene groups in the backbone of PCL chain (e.g., at 4.0 ∼ 4.1 ppm), it is judged that the terminal hydroxyl groups of the alkynyl-PCL-OH were fully reacted with isopropylidene-2,2-bis(methoxy)propionic acid, that is, the alkynyl-PCL-dioxane was successfully obtained. The deprotection of the terminal dioxane group was performed via hydrolysis in the presence of hydrochloric acid to obtain an α-alkynyl- and ω,ω′-dihydroxyl-terminated PCL. In this work, an appropriate amount of hydrochloric acid was determined to ensure that no discernable degradation of PCL chain occurred in views of the results of GPC. Notably, the signals of resonance assignable to the methylene groups in the moiety of dioxane at 3.63 and 4.19 ppm fully shifted to 3.85 and 3.68 ppm with the occurrence of the deprotection reaction, suggesting that all the dioxane moiety were transformed into dihydroxyl groups. Also shown in Figure 1 is the ^1H NMR spectrum of alkynyl-PCL$(OOCC(CH_3)_2Br)_2$.

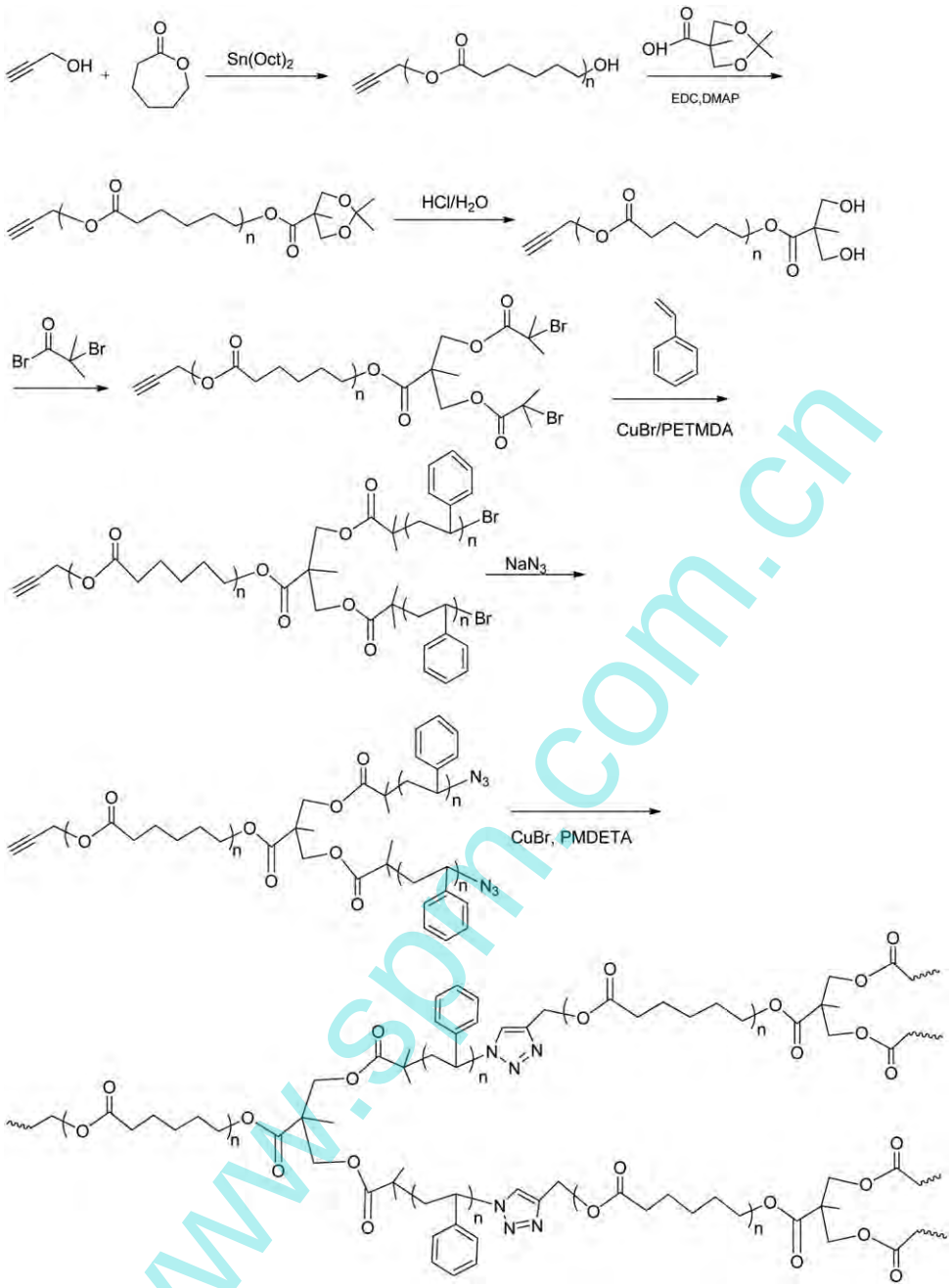

SCHEME 2 Synthesis of *h*-P[PCL-*b*-(PS)2] hyperbranched block copolymer.

Compared to the spectra of alkynyl-PCL-dioxane and alkynyl-PCL(OH)$_2$, the resonance of methyl protons in the moiety of dioxane shifted to 1.38 ppm, overlapping with the resonance of the methylene groups in the PCL chains. In addition, the peaks of resonance at 4.16 and 3.63 ppm assignable to the methylene protons of dioxane moiety completely shifted to 4.36 ppm. Concurrently, there appeared a new signal of resonance at 1.92 ppm, which is attributable to the resonance of methyl protons of 2-bromoisobutyryl groups. According to the ratio of the integral intensity of the resonance at 1.92 ppm to those of methylene protons at 4.0–4.1 ppm, it is judged that the hydroxyl groups at the ends of alkynyl-PCL(OH)$_2$ chains were fully reacted with 2-bromoisobutyryl bromide. The alkynyl-PCL[OOCC(CH$_3$)$_2$Br]$_2$ was used as the macromolecular initiator to perform the radical polymerization of styrene with the coordinate of Cu(I)Br with PMDETA as the catalyst to afford an alkynyl-PCL-*b*-(PS-Br)$_2$, the bromine atoms of which were subsequently substituted with azido groups to obtain the AB$_2$ type alkynyl-PCL-*b*-(PS-N$_3$)$_2$ macromonomer. Shown in Figure 2 are ^{1}H NMR spectra of

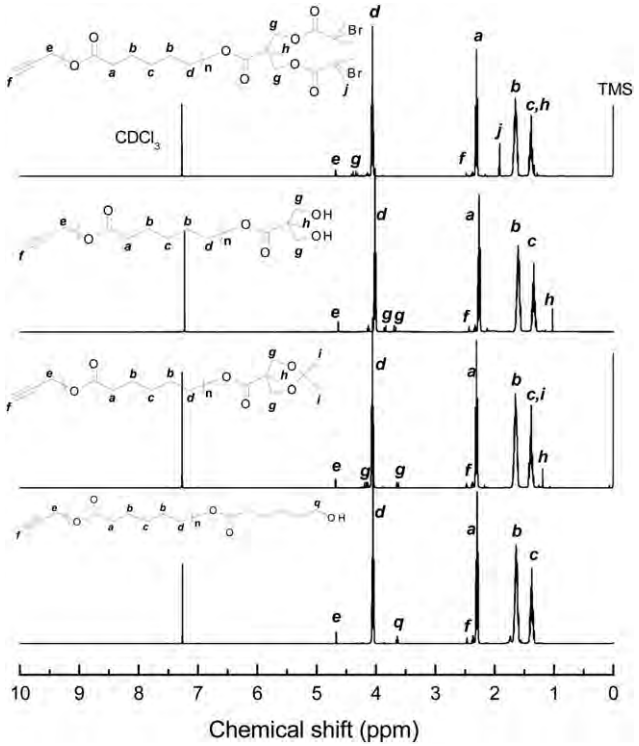

FIGURE 1 1H NMR spectra of alkynyl-PCL-OH, alkynyl-PCL-dioxane, alkynyl-PCL-OH2 and alkynyl-PCL-Br2 polymer.

the alkynyl-PCL-*b*-(PS-Br)$_2$ and alkynyl-PCL-*b*-(PS-N$_3$)$_2$. For the former, there newly appeared the signals of resonance at 1.87 and 6.2 $\sim$ 7.5 ppm, which are assignable to the protons of methine and methylene groups in the main chain and aromatic rings of polystyrene. Notably, the resonance of the protons of methine connected to bromine atom at the ends of PS chains were detected at 4.35 $\sim$ 4.55 ppm. After the bromine atoms were substituted by azido groups, this resonance completely shifted to 4.95 $\sim$ 4.05 ppm, suggesting that all the bromine atoms of alkynyl-PCL-*b*-(PS-Br)$_2$ were substituted by azido groups. This observation indicates that the alkynyl-PCL-*b*-(PS-N$_3$)$_2$ was successfully obtained.

Synthesis of Hyperbranched Block Copolymer

The above AB$_2$ macromonomer, alkynyl-PCL-*b*-(PS-N$_3$)$_2$ was subjected to the polymerization via a copper-catalyzed Huisgen 1,3-dipolar cycloaddition reaction. The viscosity of the system gradually increased with increasing the time of polymerization, indicative of the occurrence of the polymerization. Also shown in Figure 2 is the ^{1}H NMR spectrum of the polymerized product. The resonance peaks of the protons assignable to PCL chains were clearly exhibited at 1.38, 1.65, 2.30, and 4.05 ppm, assignable to the protons of methylene groups of PCL subchains as indicated in this spectrum. In addition, the signals of proton resonance for PS subchains were detected at 1.38 and 1.84 ppm, assignable to the protons of methylene and methine groups in PS main chains; the peaks of resonance in the range of 7.3–6.3 ppm were attributable to the protons of aromatic rings of PS subchains. The ^{1}H NMR spectroscopy showed that the resulting copolymer combined the structural features from PS and PCL subchains. The FTIR spectra of the AB$_2$ macromonomer and hyperbranched block copolymer are shown in Figure 3. For the AB$_2$ macromonomer, the band at 2099 cm^{-1} is assignable to the stretching vibration of azido group. For the hyperbranched block copolymer, this band completely disappeared, indicating the efficiency of the polymerization via click chemistry. Shown in Figures 4 and 5 are the GPC curves of the AB$_2$ macromonomer and the product after the macromonomer was polymerized for 72 h. For the macromonomer, the unimodal peaks was displayed in all the GPC measurements. While the GPC measurement was performed with DMF as eluent and with a RI detector, the molecular weight was measured to be M_n = 5700 Da with M_w/M_n=1.16, relative to PS standards. While the GPC measurement was carried out on an apparatus equipped with a light scattering detector and with THF as the eluent, the molecular weight was measured to be M_n = 4800 Da with M_w/M_n=1.16. In terms of the length of PCL subchain (viz. M_{PCL} = 2300 Da) determined by means of ^{1}H NMR spectroscopy, the length of PS subchains were calculated to be M_{PS} = 1300 Da and thus the mass fraction of PS in the macromonomer was calculated to be f_{PS} = 0.52. For the polymerized product, a bimodal distribution of molecular weight was exhibited. Notably, the peak at the retention time of t = 20 min was attributable to the AB$_2$ macromonomer, suggesting that there still was the AB$_2$ macromonomer in the polymerized product. The result of curve deconvolution showed that there was about 16 % of the

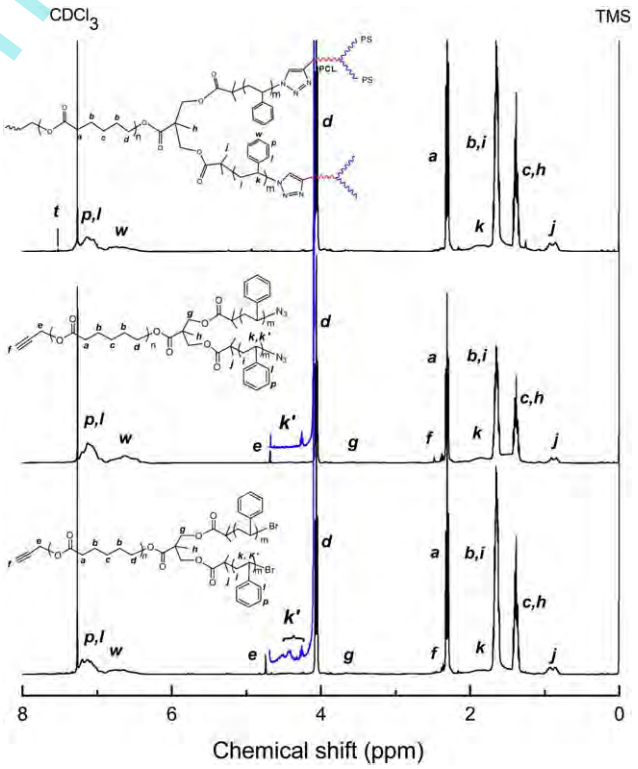

FIGURE 2 1H NMR spectra of PCL-*b*-(PS-Br)2, PCL-*b*-(PS-N3)2 macromonomers and *h*-P[PCL-*b*-(PS)2]. [Color figure can be viewed in the online issue, which is available at wileyonlinelibrary.com.]

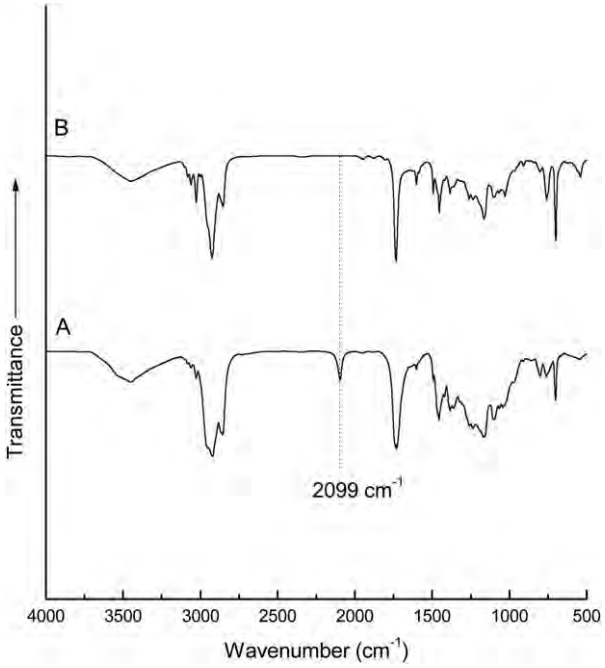

FIGURE 3 FTIR spectra of: A) PCL-*b*-(PS-Br)2 macromonomer and B) *h*-P[PCL-*b*-(PS)2] block copolymer.

macromonomer left in the polymerized product. Owing to the big difference in molecular weights between the hyperbranched block copolymer and the macromonomer, the AB_2

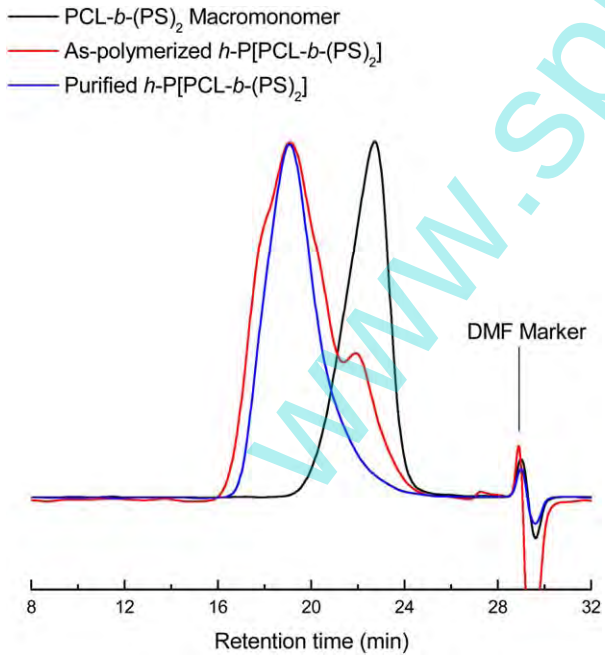

FIGURE 4 GPC curves of PCL-*b*-(PS-Br)2 macromonomer and *h*-P[PCL-*b*-(PS)2] block copolymer. The GPC measurement was carried out with DMF as eluent and with RI detectors and the molecular weight was expressed with PS standard. [Color figure can be viewed in the online issue, which is available at wileyonlinelibrary.com.]

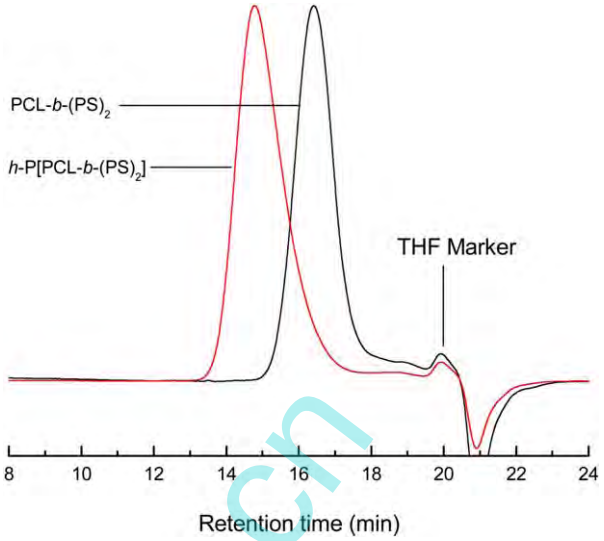

FIGURE 5 GPC curves of PCL-*b*-(PS-Br)2 macromonomer and *h*-P[PCL-*b*-(PS)2] block copolymer. The GPC measurement was carried out with THF as eluent and with light scattering detectors. [Color figure can be viewed in the online issue, which is available at wileyonlinelibrary.com.]

macromonomer was readily removed by adding precipitant (e.g., petroleum ether) into the dichloromethane solution of the hyperbranched block copolymer. After removal of the AB_2 macromonomer, the product displayed a unimodal distribution of molecular weight (See Figs. 4 and 5). While the GPC measurement was performed with DMF as eluent and with a RI detector, the molecular weight was measured to be M_n = 71,300 with M_w/M_n=1.43, relative to PS standards. While the GPC measurement was carried out on an apparatus equipped with a light scattering detector and with THF as the eluent, the molecular weight was measured to be M_n = 78,600 with M_w/M_n = 1.37. It is seen that the molecular weight value of the hyperbranched block copolymer measured with light scattering detector and with THF eluent was slightly higher than that with RI detector and with DMF eluent, relative to PS standard. Nonetheless, the results of ^{1}H NMR and GPC indicate that the hyperbranched block copolymer composed of PS and PCL subchains (denoted *h*-P[PCL-*b*-$(PS)_2$]) was successfully obtained.

The hyperbranched block copolymer, *h*-P[PCL-*b*-$(PS)_2$] was subjected to differential scanning calorimetry (DSC) to investigate the possible microphase separation in the copolymer. Shown in Figure 6 are the DSC curves of the sample with different thermal treatments. For the sample annealed at 40°C for two weeks, a glass transition at 112°C and an endothermic transition at about 70°C were exhibited (See curve A in Fig. 6). The former is attributable to PS subchain whereas the letter to the melting of PCL subchains. Owing to the isothermal crystallization at 40°C for a very long time (viz. two weeks), the measured value of the melting point of PCL microdomains ($T_m \approx 70$°C) was quite close to the equilibrium melting points reported in literature.[56] The fact that the melting of PCL subchains appeared ahead of the glass transition of PS subchains indicates that the hyperbranched

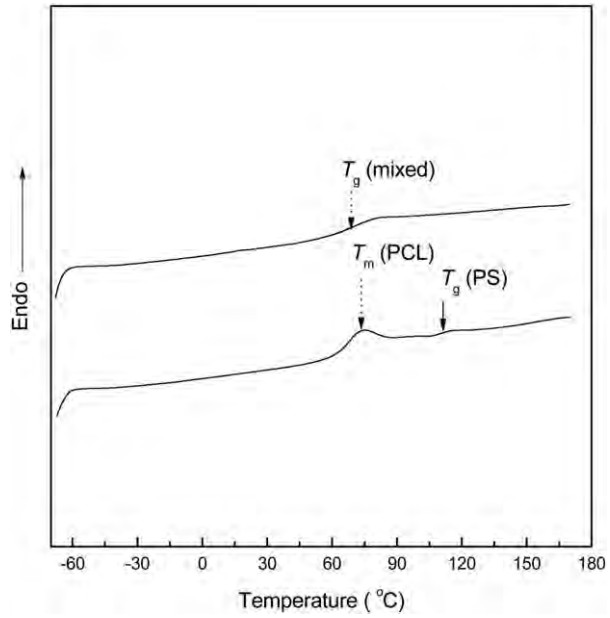

FIGURE 6 DSC curves of *h*-P[PCL-*b*-(PS)2].

block copolymer was microphase-separated. After the sample was molten at 170°C for 5 min and then quenched to −70°C, the microphase-separated morphology disappeared as evidenced by the observation that only one single glass transition was displayed (See curve B in Fig. 6). This observation can be accounted for by the upper-critical solution temperature (UCST) in the blends of PS and PCL.[57,58] The microphase-separated morphology of the hyperbranched block copolymer was investigated by means of AFM. Shown in Figure 7 is the AFM phase image of the sample. In terms of the difference in viscoelasticity between PS and PCL subchains, the dark regions are attributable to PCL microphases and the light to PS microphases. Notably, a bicontinuous microphase-separated morphology was displayed for the hyperbranched block copolymer. The microphase-separated morphology was in good agreement with the result of DSC. The results of DSC and AFM indicate that the hyperbranched block copolymer was microphase-separated.

Reaction-Induced Microphase Separation in Epoxy Thermosets

In the past years, there have been several reports on the formation of the nanophases in epoxy thermosets by the use of the binary block copolymers composed of PS and PCL subchains.[40,59] In these previous reports, the copolymers had linear AB diblock or ABA triblock architectures. To the best of our knowledge, a block copolymer with hyperbranched architecture has not been used to investigate the formation of nanophases in epoxy thermosets. In this work, we explore to incorporate the hyperbranched block copolymer, *h*-P[PCL-*b*-$(PS)_2$] into epoxy to access the nanostructured thermosets.

All the mixtures composed of the precursors of epoxy (viz. DGEBA + MOCA) and the *h*-P[PCL-*b*-$(PS)_2$] were transparent, suggesting that the mixtures were homogeneous before the curing reaction, suggesting that no macroscopic phase separation occurred. The mixtures were cured at elevated temperature to obtain the thermosets. Notably, all the cured thermosets containing *h*-P[PCL-*b*-$(PS)_2$] were also homogenous and transparent, indicating that no macroscopic phase separation occurred in the process of the curing reaction. Nonetheless, microphase separation cannot be excluded since the PS subchains of the hyperbranched block copolymer were prone to demixing out of the epoxy network via reaction-induced microphase separation mechanism. The epoxy thermosets were subjected to the morphological observation by means of AFM. Shown in Figure 8 are the AFM phase images of the thermosets containing various contents of *h*-P[PCL-*b*-$(PS)_2$]. In all the cases, the microphase-separated morphologies were exhibited. The dark region is attributable to PS microphases whereas the light to the epoxy matrix in views of the difference in viscoelasticity between epoxy matrix and PS. For the thermoset containing 10 wt % of *h*-P[PCL-*b*-$(PS)_2$], both spherical and worm-like PS microdomains with the size of 20–30 nm in diameter were dispersed in the continuous epoxy matrix [See Fig. 8(A)]. The fraction of the worm-like PS microdomains significantly increased with increasing the content of *h*-P[PCL-*b*-$(PS)_2$]. The AFM results indicate that the nanostructures were indeed formed while the hyperbranched block copolymer was incorporated into epoxy. The formation of nanophases were further confirmed by means of SAXS. The SAXS profiles of the thermosets are shown in Figure 9. The thermosets displayed the scattering phenomenon and the scattering intensity increased with increasing the content of *h*-P[PCL-*b*-$(PS)_2$]. It is seen that the scattering peaks slightly shifted to the positions with higher *q* values with increasing the content of the hyperbranched block copolymer. The SAXS results indicate that all the thermosets investigated were

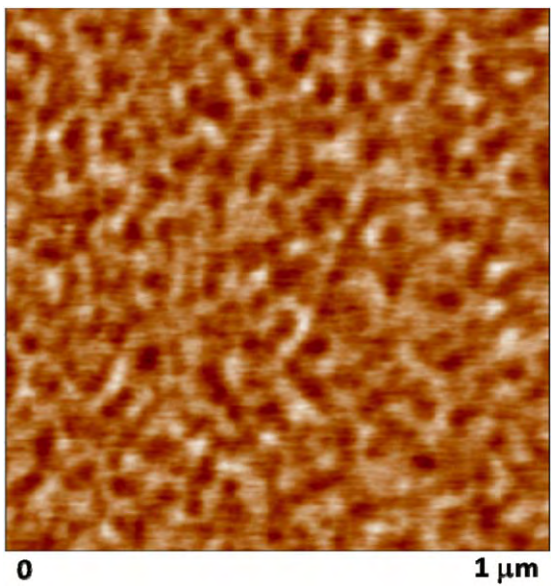

FIGURE 7 AFM phase images of *h*-P[PCL-*b*-(PS)2]. [Color figure can be viewed in the online issue, which is available at wileyonlinelibrary.com.]

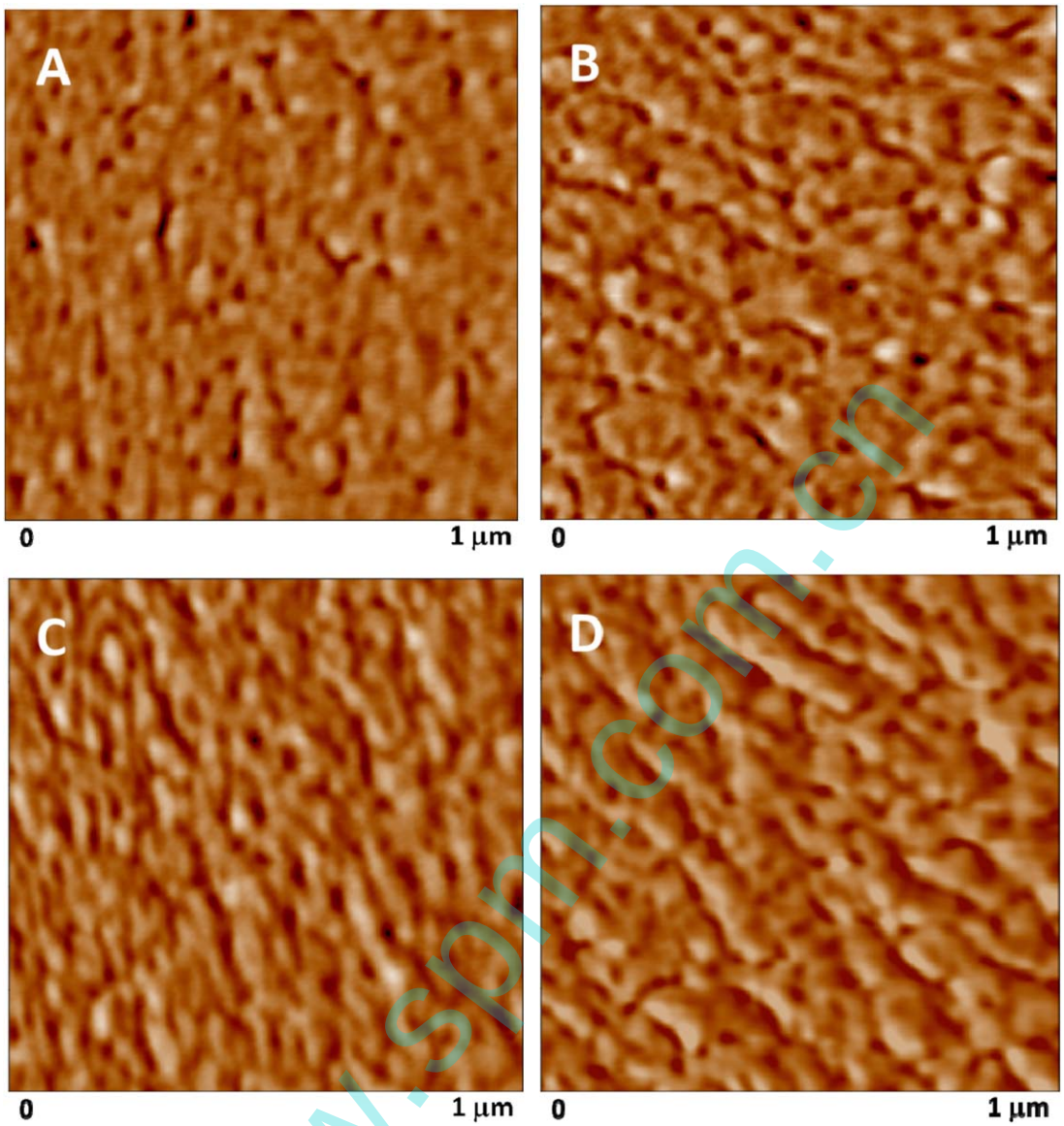

FIGURE 8 AFM phase images of the epoxy thermosets containing (A) 10, (B) 20, (C) 30, and (D) 40 wt % of *h*-P[PCL-*b*-(PS)2]. [Color figure can be viewed in the online issue, which is available at wileyonlinelibrary.com.]

indeed microphase-separated, which was in good agreement with the AFM results. To investigate the formation mechanism of the nanostructures in epoxy thermosets, the mixtures of the precursors of epoxy (i.e., DGEBA + MOCA) with the hyperbranched block copolymer were subjected to small angle X-ray scattering (SAXS) after and before the curing reaction. Representatively shown in Figure 10 are the SAXS profiles of the ternary mixture composed of DGEBA, MOCA and 40 wt% of *h*-P[PCL-*b*-$(PS)_2$]. At room and the curing temperature (viz. 150°C), no scattering peak was exhibited, indicating that the mixture was homogenous. After cured at 150°C for 3 h, however, the scattering peak appeared. The appearance of the scattering peak indicates that the reaction-induced microphase separation occurred. The results of SAXS showed that the formation of nanophases in the thermoset containing *h*-P[PCL-*b*-$(PS)_2$] hyperbranched block copolymer followed the reaction-induced microphase separation mechanism.

The above nanostructured thermosets containing the *h*-P[PCL-*b*-$(PS)_2$] hyperbranched block copolymer were subjected to dynamic mechanical thermal analysis (DMTA) and the DMTA spectra are shown in Figure 11. For the control epoxy, a major transition (viz. α-transition) was exhibited at *c.a.* 159°C and it was responsible for the glass-rubber transition of the crosslinked polymer. Apart from the α-transition, the crosslinked network exhibited the secondary transitions (viz. β-transition) at approximately −56 and 73°C, respectively. The former is attributed predominantly to the motion of hydroxyl ether structural units [-$CH_2CH(OH)CH_2O$-] in amine-cross linked epoxy whereas the latter to that of diphenyl groups in the backbone of epoxy network.[60,61]

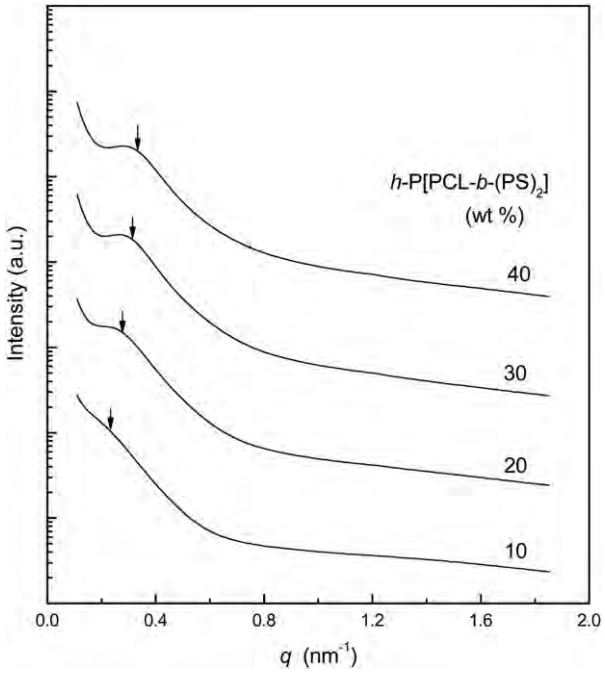

FIGURE 9 SAXS profiles of the epoxy thermosets containing *h*-P[PCL-*b*-(PS)2].

Upon adding *h*-P[PCL-*b*-$(PS)_2$], the α-transitions were observed to shift to lower temperature; the transition temperatures were decreased with increasing the content of *h*-P[PCL-*b*-$(PS)_2$]. The α-transition temperature was decreased to 99°C while the content of *h*-P[PCL-*b*-$(PS)_2$] was 40 wt %.

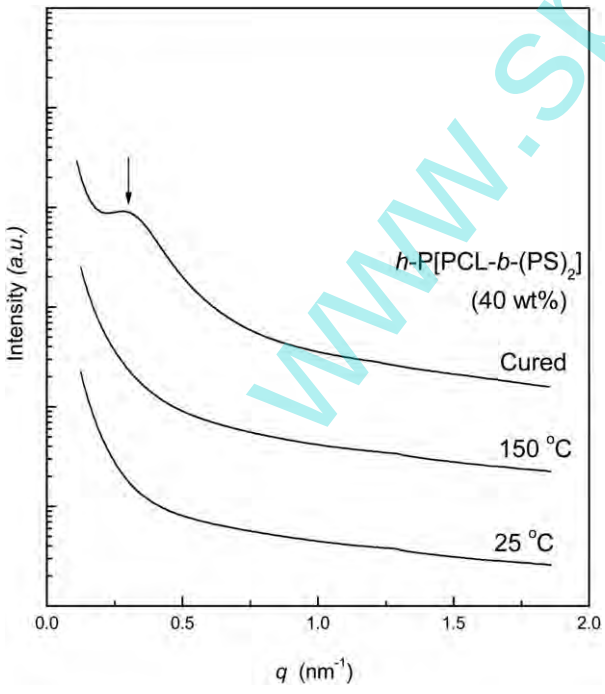

FIGURE 10 SAXS profiles of the epoxy thermosets containing 40% of *h*-P[PCL-*b*-(PS)2]: A) at 25°C; B) at 150°C; C) after cured at 150°C for 3 h plus 180°C for 2 h.

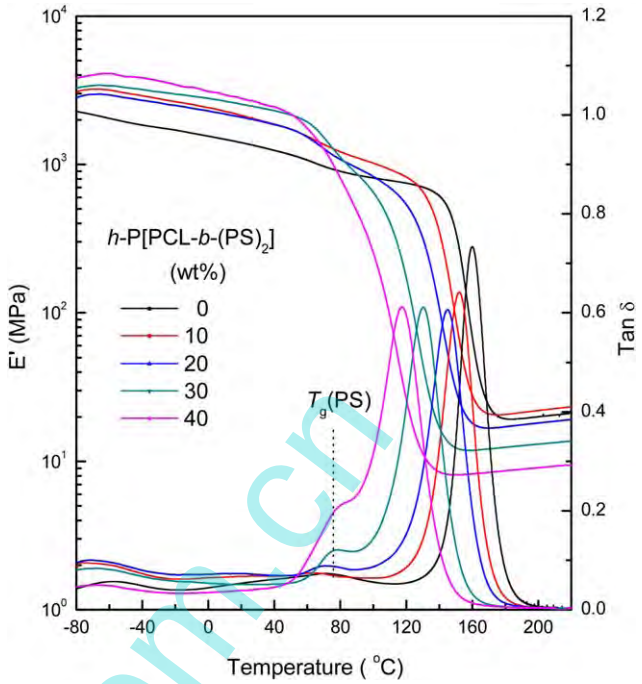

FIGURE 11 DMTA curves of the epoxy thermosets containing 10, 20, 30 and 40 wt % of *h*-P[PCL-*b*-(PS)2]. [Color figure can be viewed in the online issue, which is available at wileyonlinelibrary.com.]

The decreased α-transition temperatures were attributable to the plasticization effect of the PCL blocks which possessed the T_g as low as −65°C on epoxy matrices. In other word, the PCL subchains remained mixed with epoxy network at the segmental level. For the thermosets containing *h*-P[PCL-*b*-$(PS)_2]_n$, there were additionally the major transitions at about 100°C, the intensity of which increased with increasing the content of *h*-P[PCL-*b*-$(PS)_2]_n$. These transitions are assignable to the PS microdomains. It is noted that the transition temperatures of the PS microdomains remained almost invariant irrespective of the content of *h*-P[PCL-*b*-$(PS)_2$]. The appearance of the major transitions assignable to PS and epoxy network indicates that the PS microdomains were indeed formed, i.e., the PS subchains of the hyperbranched block copolymer were demixed out of the mixtures with epoxy matrix.

CONCLUSIONS

In this work, we have successfully synthesized a novel hyperbranched block copolymer composed of PCL and PS subchains via the combination of ring-opening polymerization, ATRP and copper-catalyzed Huisgen 1,3-dipolar cycloaddition (i.e., click chemistry) polymerization. First, we synthesized an α-alkynyl- and ω,ω′-diazido-terminated AB_2 PCL-*b*-$(PS)_2$ macromonomer via the combination of ROP and ATRP. The synthesis of the *h*-P[PCL-*b*-$(PS)_2]_n$ hyperbranched block copolymer was carried out via a copper-catalyzed Huisgen 1,3-dipolar cycloaddition (i.e., click reaction) polymerization of the AB_2 macromonomer and a high-molecular weight product was obtained as evidenced by means of ^1H

nuclear magnetic resonance (NMR) spectroscopy and GPC. Both DSC and AFM showed that the *h*-P[PCL-*b*-$(PS)_2]_n$ hyperbranched block copolymer was microphase-separated. Incorporating the hyperbranched block copolymer into epoxy afforded the nanostructured thermosets. The formation of nanophases in epoxy was investigated by means of SAXS, atomic force AFM and DMTA. It was found that the formation of the nanophases in the thermosets followed reaction-induced microphase separation mechanism.

ACKNOWLEDGMENTS

The financial supports from Natural Science Foundation of China (No. 51133003 and 21274091) were gratefully acknowledged. The authors thank the Shanghai Synchrotron Radiation Facility for the support under the projects of Number 13SRBL16B14042.

REFERENCES AND NOTES

1 D. Mecerreyes, R. Jérôme, P. Dubois, In Macromolecular Architectures; Springer Verlag, Berlin, **1999**; pp 1-59.

2 A. Sunder, J. Heinemann, H. Frey, *Chem.: Eur. J.* **2000**, *6*, 2499-2506.

3 M. Jikei, M.-A. Kakimoto, *Prog. Polym. Sci.* **2001**, *26*, 1233-1285.

4 C. Gao, D. Yan, *Prog. Polym. Sci.* **2004**, *29*, 183-275.

5 M. G. McKee, S. Unal, G. L. Wilkes, T. E. Long, *Prog. Polym. Sci.* **2005**, *30*, 507-539.

6 M. Trollsås, J. L. Hedrick, *Macromolecules* **1998**, *31*, 4390-4395.

7 M. Trollsås, P. Löwenhielm, V. Lee, M. Möller, R. Miller, J. Hedrick, *Macromolecules* **1999**, *32*, 9062-9066.

8 L. R. Hutchings, J. M. Dodds, S. J. Roberts-Bleming, *Macromolecules* **2005**, *38*, 5970-5980.

9 L. R. Hutchings, J. M. Dodds, S. J. Roberts-Bleming, *Macromolecular Symp.*, **2006**, *240*, 56-67.

10 J. Xu, L. Tao, J. Liu, V. Bulmus, T. P. Davis, *Macromolecules* **2009**, *42*, 6893-6901.

11 L. Z. Kong, M. Sun, H. M. Qiao, C. Y. Pan, *J. Polym. Sci., Part A: Polym. Chem.* **2010**, *48*, 454-462.

12 J. M. Frechet, M. Henmi, I. Gitsov, S. Aoshima, M. R. Leduc, R. B. Grubbs, *Science* **1995**, *260*, 1080-1080.

13 C. J. Hawker, J. M. Frechet, R. B. Grubbs, J. Dao, *J. Am. Chem. Soc.* **1995**, *117*, 10763-10764.

14 M. Liu, N. Vladimirov, J. M. Fréchet, *Macromolecules* **1999**, *32*, 6881-6884.

15 H. Magnusson, E. Malmström, A. Hult, *Macromol. Rapid Commun.* **1999**, *20*, 453-457.

16 S. Peleshanko, R. Gunawidjaja, S. Petrash, V. Tsukruk, *Macromolecules* **2006**, *39*, 4756-4766.

17 W.-J. Wang, D. Wang, B.-G. Li, S. Zhu, *Macromolecules* **2010**, *43*, 4062-4069.

18 M. Trollsås, M. A. Kelly, H. Claesson, R. Siemens, J. L. Hedrick, *Macromolecules* **1999**, *32*, 4917-4924.

19 L. Li, X. Wang, C. He, W. He, *J. Polym. Sci., Part A: Polym. Chem.* **2014**, *52*, 128-138.

20 M. A. Hillmyer, P. M. Lipic, D. A. Hajduk, K. Almdal, F. S. Bates, *J. Am. Chem. Soc.* **1997**, *119*, 2749-2750.

21 P. M. Lipic, F. S. Bates, M. A. Hillmyer, *J. Am. Chem. Soc.* **1998**, *120*, 8963-8970.

22 F. Meng, S. Zheng, W. Zhang, H. Li, Q. Liang, *Macromolecules* **2006**, *39*, 711-719.

23 F. Meng, S. Zheng, H. Li, Q. Liang, T. Liu, *Macromolecules* **2006**, *39*, 5072-5080.

24 J. Mijovic, M. Shen, J. W. Sy, I. Mondragon, *Macromolecules* **2000**, *33*, 5235-5244.

25 R. B. Grubbs, J. M. Dean, M. E. Broz, F. S. Bates, *Macromolecules* **2000**, *33*, 9522-9534.

26 R. B. Grubbs, J. M. Dean, F. S. Bates, *Macromolecules* **2001**, *34*, 8593-8595.

27 Q. Guo, R. Thomann, W. Gronski, T. Thurn-Albrecht, *Macromolecules* **2002**, *35*, 3133-3144.

28 S. Ritzenthaler, F. Court, L. David, E. Girard-Reydet, L. Leibler, J. Pascault, *Macromolecules* **2002**, *35*, 6245-6254.

29 S. Ritzenthaler, F. Court, E. Girard-Reydet, L. Leibler, J. Pascault, *Macromolecules* **2003**, *36*, 118-126.

30 V. Rebizant, V. Abetz, F. Tournilhac, F. Court, L. Leibler, *Macromolecules* **2003**, *36*, 9889-9896.

31 V. Rebizant, A.-S. Venet, F. Tournilhac, E. Girard-Reydet, C. Navarro, J.-P. Pascault, L. Leibler, *Macromolecules* **2004**, *37*, 8017-8027.

32 J. M. Dean, N. E. Verghese, H. Q. Pham, F. S. Bates, *Macromolecules* **2003**, *36*, 9267-9270.

33 I. Zucchi, M. Galante, R. Williams, *Polymer* **2005**, *46*, 2603-2609.

34 Y. S. Thio, J. Wu, F. S. Bates, *Macromolecules* **2006**, *39*, 7187-7189.

35 E. Serrano, A. Tercjak, G. Kortaberria, J. A. Pomposo, D. Mecerreyes, N. E. Zafeiropoulos, M. Stamm, I. Mondragon, *Macromolecules* **2006**, *39*, 2254-2261.

36 C. Ocando, E. Serrano, A. Tercjak, C. Pena, G. Kortaberria, C. Calberg, B. Grignard, R. Jerome, P. M. Carrasco, D. Mecerreyes, *Macromolecules* **2007**, *40*, 4068-4074.

37 S. Maiez-Tribut, J.-P. Pascault, E. Soule, J. Borrajo, R. J. Williams, *Macromolecules* **2007**, *40*, 1268-1273.

38 C. Sinturel, M. Vayer, R. Erre, H. Amenitsch, *Macromolecules* **2007**, *40*, 2532-2538.

39 Z. Xu, S. Zheng, *Macromolecules* **2007**, *40*, 2548-2558.

40 F. Meng, Z. Xu, S. Zheng, *Macromolecules* **2008**, *41*, 1411-1420.

41 C. Ocando, A. Tercjak, M. D. Martín, J. A. Ramos, M. Campo, I. Mondragon, *Macromolecules* **2009**, *42*, 6215-6224.

42 W. Fan, L. Wang, S. Zheng, *Macromolecules* **2010**, *43*, 10600-10611.

43 E. Serrano, M. Larrañaga, P. M. Remiro, I. Mondragon, P. M. Carrasco, J. A. Pomposo, D. Mecerreyes, *Macromol. Chem. Phys.* **2004**, *205*, 987-996.

44 E. Serrano, M. D. Martin, A. Tercjak, J. A. Pomposo, D. Mecerreyes, I. Mondragon, *Macromol. Rapid Commun.* **2005**, *26*, 982-985.

45 R. Yu, S. Zheng, X. Li, J. Wang, *Macromolecules* **2012**, *45*, 9155-9168.

46 C. Zhang, L. Li, S. Zheng, *Macromolecules* **2013**, *46*, 2740-2753.

47 H. N. E. Romeo, I. A. Zucchi, M. Rico, C. E. Hoppe, R. J. Williams, *Macromolecules* **2013**, *46*, 4854-4861.

48 D. Hu, Z. Xu, K. Zeng, S. Zheng, *Macromolecules* **2010**, *43*, 2960-2969.

49 M. A. Amendt, L. Chen, M. A. Hillmyer, *Macromolecules* **2010**, *43*, 3924-3934.

50 L. Zhu, C. Zhang, J. Han, S. Zheng, X. Li, *Soft Matter* **2012**, *8*, 7062-7072

51 M. Yin, S. Zheng, *Macromol. Chem. Phys.* **2005**, *206*, 929-937.

52 Y. Ni, S. Zheng, *Polymer* **2005**, *46*, 5828-5839.

53 C. Hoppe, M. Galante, P. Oyanguren, R. Williams, E. Girard-Reydet, J.-P. Pascault, *Polym. Eng. Sci.* **2002**, *42*, 2361-2368.

54 I. A. Zucchi, M. J. Galante, J. Borrajo, R. J. Williams, *Macromol. Chem. Phys.* **2004**, *205*, 676-683.

55 L. Li, C. He, W. He, C. Wu, *Macromolecules* **2011**, *44*, 8195-8206.

56 S. Zheng, H. Zheng, Q. Guo, *J. Polym. Sci., Part B: Polym. Phys.* **2003**, *41*, 1085-1098.

57 Y. Li, B.-J. Jungnickel, *Polymer* **1993**, *34*, 9-15.

58 J. S. Oh, J. G. Jang, Y. C. Bae, *Polymer* **1997**, *38*, 3761-3766.

59 R. Yu, S. Zheng, *Macromolecules* **2011**, *44*, 8546-8557.

60 L. Robeson, *Polym. Eng. Sci.* **1969**, *9*, 277-281.

61 A. A. Jones, *Macromolecules* **1985**, *18*, 902-906.